Desalination and Water Treatment
www.deswater.com
doi: 10.1080/19443994.2015.1076353

57 (2016) 16066–16077
July

Taylor & Francis
Taylor & Francis Group

Integrated air stripping and non-thermal plasma system for the treatment of volatile organic compounds from wastewater: statistical optimization

Mohammed Evuti Abdullahi[a,*], Mohd Ariffin Abu Hassan[b], Zainura Zainon Noor[b], R.K. Raja Ibrahim[c]

[a]*Department of Chemical Engineering, University of Abuja, Abuja, Nigeria, Tel. +234 8036200828; email: evutimohd@yahoo.com*
[b]*Institute of Environmental and Water Resources Management, Universiti Teknologi Malaysia, Johor Bahru 81310, Malaysia, email: mariffin@utm.my (M.A. Abu Hassan), zainurazn@utm.my (Z. Zainon Noor)*
[c]*Faculty of Science, Physics Department, Advanced Photonic Science Institute, Universiti Teknologi, Johor Bahru 81310, Malaysia, email: rkamarulzaman@utm.my*

Received 9 January 2015; Accepted 15 July 2015

ABSTRACT

This study examined the treatment of toluene and m-xylene from wastewater using integrated air stripping and non-thermal plasma (NTP) reactor system. Toluene and m-xylene concentrations, before and after plasma treatment, were determined using Fourier transform infrared spectroscopy. The performance of the NTP reactor was optimized using the central composite design of the response surface methodology. The optimum discharge gap, applied voltage, and flow rate for the decomposition were found to be 22.34 mm, 15 kV, 3.56 L/min and 20.10 mm, 15 kV, 3.34 L/min for toluene and m-xylene, respectively. Experimental removal efficiencies and model predictions were in close agreement with 1.25 and 2.16% errors for toluene and m-xylene, respectively. The developed model could fit the experimental data with acceptable values of percentage errors.

Keywords: Wastewater; Volatile organic compounds; Air stripper; Non-thermal plasma reactor; Response surface methodology

1. Introduction

Effluents from industries, contaminated groundwater, and hazardous landfill leachate release volatile organic compounds (VOCs), such as toluene and m-xylene, into the surrounding [1]. The negative effects of VOCs include stratospheric ozone depletion, ground level photochemical ozone formation, toxic or carcinogenic human health effects, enhancing the global greenhouse effect, and accumulation and persistence in the environment [1–4]. Studies have shown that an economical solution to VOCs removal from wastewater can be best achieved using a combination of technologies [5]. Based on this, different scenarios of the treatment of the VOCs from wastewater have been carried out. These include combination of non-thermal plasma (NTP) reactor and biotrickling filter and decontamination of groundwater using air stripping and oxidation of the VOCs [5,6]. Air stripping is a technology that uses an air stripper for VOCs removal from wastewater by increasing the surface area of the contaminated water that is exposed to air. It is widely used for the removal of VOCs from wastewater in the process industries. However, air

*Corresponding author.

stripping is only a mere phase separation and the off-gas from the air stripper may have to undergo further treatment to meet the emission limits [6].

Optimization refers to manipulating the most important process variables to levels or settings that result in the best obtainable set of operating conditions for the system or process [7]. The decomposition of VOCs in NTP is a complex process associated with sensitivity to slight changes in the operation parameters. This usually affects the type and quantity of the by-product formation; hence, the reactor performance efficiency. Several studies have investigated the influence of operating parameters on the efficiency of the NTP reactor. In general, the efficiency has been found to depend on carrier gas flow rate, gap distance between electrodes, applied voltage, shape and size of ferroelectric material, and their dielectric constant among others [8–12]. Therefore, there is a need for a simultaneous optimization of these (often conflicting) responses. Different researchers had ventured into many ways of optimizing the NTP reactor performance. This involves changing the levels of one factor while keeping the others constant, running the experiment, observing the results, and then moving on to the next factor. This is indeed time and energy consuming. It is also usually incapable of revealing the optimal combination of factors since the interaction among them has been ignored [13,14]. Statistical experimental design allows for better and easier analysis of data. This technique permits us to get the maximum information from a limited number of experiments and to represent the behavior of a particular system by mathematical models [8,15]. Using graphic representations of the models via the response surface, the researcher is able to visualize the complete behavior of the system under study. Moreover, the response of the system can be predicted for values of the factors that were not assayed (within the selected range for the variables). Most probably, it is possible to predict the conditions to get a better performance or at least to get a system less sensitive to the unpredicted variations of the operative variables. These models must correlate with target parameters, such as efficiency or yield, with those variables that may exert influence over them [8].

The response surface methodology (RSM) involves mathematics and statistical techniques that can predict, how a target response (selected response of interest) is influenced by many variables. RSM includes the influences of individual factors as well as the influences of their combined action. An interaction means that the effect that one variable can exert on the system will depend on the values of the rest of variables [8]. RSM is a technique for designing experiments, building models, evaluating the effects of several factors, and achieving the optimum conditions for desirable responses with a limited number of planned experiments [14,16,17]. RSM therefore, is an extremely useful framework for modeling and optimizing system [7]. Moreover, complete theoretical models are frequently not available and sometimes any attempt to develop one could not be justified from an economic point of view [9].

RSM has been widely used to optimize products and processes in many fields, such as biotechnology [17], water and wastewater treatment [13,14], plasma surface coating [18], polymer fabrication [19], and in the development of new processes [16]. However, only few reported works are available in the area of NTP [8,9]. This study examined the treatment of toluene and m-xylene from wastewater using integrated air stripping and NTP reactor system. Toluene and m-xylene concentrations before and after plasma treatment were determined using the Fourier transform infrared spectroscopy. The performance of a NTP reactor was optimized using the central composite design (CCD) of the RSM.

2. Experimental

2.1. Materials

Toluene and m-xylene were obtained from Merck Sdn Bhd, Malaysia with greater than 99.5% purity. Synthetic wastewater containing 1,500 ppm of toluene and m-xylene was prepared. The experimental setup is shown in Fig. 1. It consists of a custom-made pilot-scale packed column air stripper (Model 2T4H) from Branch Environmental Corporation USA, made of a 1.5-m stainless steel tube of 0.05-m internal diameter filled with 6 mm-ceramic raschig ring packing. The height of the packing is 1.15 m, which is equivalent to a packing volume of 2.26×10^{-3} m^3. The ferroelectric-packed bed NTP reactor consists of a Pyrex glass tube of 1-inch internal diameter and standard length and 3-mm diameter barium Titanate ($BaTiO_3$) pellets (dielectric constant of 10,000) from Fuji Titanium Industry Co. Ltd, Japan as dielectric material packed in between the two electrodes made from stainless steel. The electrodes and $BaTiO_3$ pellets were supported with two-funnel head stainless steel tubes. O-rings smeared with vacuum grease were used to fix the packed bed in between the two mesh electrodes and to ensure that it is properly sealed. Teflon caps equipped with O-rings were then used to seal both ends of the Pyrex tube to create a properly confined area in the Pyrex tube. High-voltage electric connectors were fixed to the two ends of the stainless steel

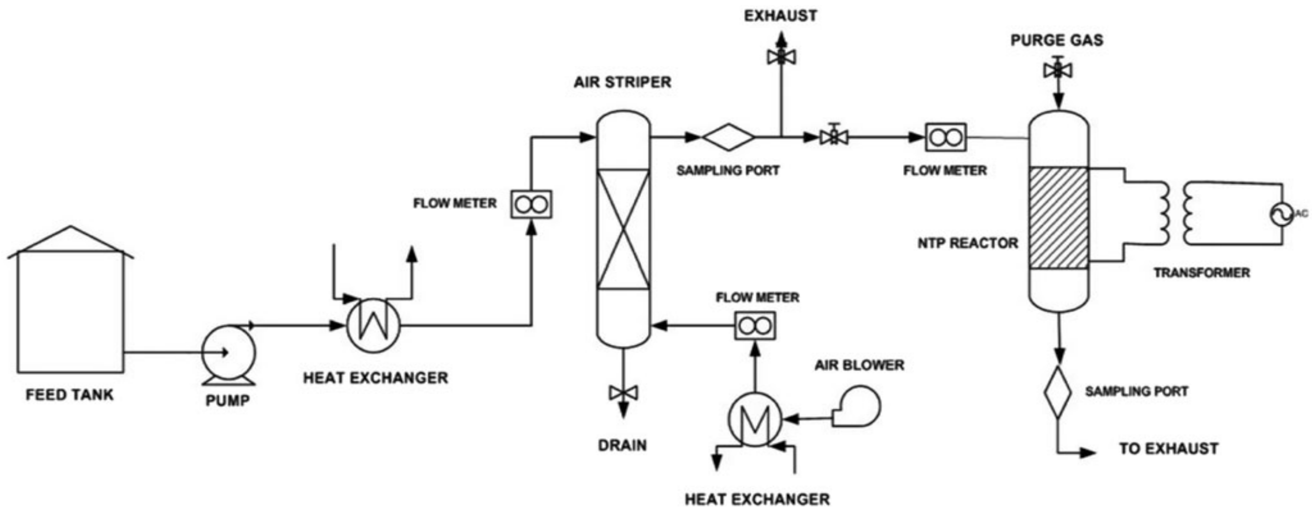

Fig. 1. Process flow diagram of the integrated air stripping–NTP reactor system.

tube. The plasma reactor was powered with a 20-kV/3 Amp AC power supply transformer with input power of 240 V and 50-Hz frequency. This is further illustrated by a schematic drawing of the ferroelectric-packed NTP reactor shown in Fig. 2.

2.2. Methods

To remove toluene and m-xylene from the wastewater using the air stripper, the air flow rate and inlet wastewater were set at 7.08 L/min and 0.12 L/min, respectively, using a rotameter. The wastewater and air heaters were set at 50˚C. The air and contaminated water were then pumped into the air stripper in a counter-current operation. The treated wastewater was collected at the bottom while VOC-rich air exiting at the top of the column was sent to the NTP reactor. The effect of applied voltage, flow rate, and discharge gap on the decomposition of toluene and m-xylene was studied by operating the NTP reactor at different conditions according to the experimental plan using Design expert 7.0 software. A

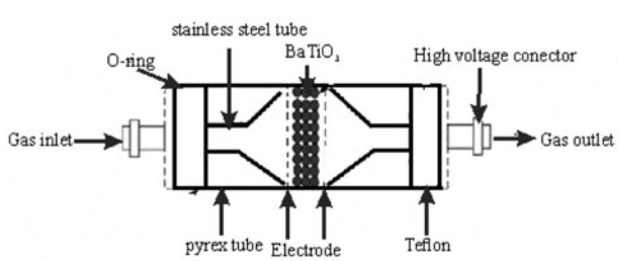

Fig. 2. Schematic drawing of the ferroelectric-packed NTP reactor.

high-voltage probe was used to measure the applied voltage and the current was measured using digital Pico scope.

Toluene and m-xylene concentrations in the outlet gas from the air stripper were first determined with a Frontier FT-IR spectrometer (Perkin Elmer) coupled with cyclone gas cell accessory (Cyclone™ C5) manufactured by Specac Ltd., using nitrogen gas as a background measurement. The gas streams were passed into multiple pass optical gas cell (Specac Ltd) with a white-type mirror arrangement with an optical path length set at 8 m. Sample spectrum for each operating condition was captured after 15 min at room temperature and atmospheric pressure at a spectra resolution of 1 cm^{-1}. The number of FTIR scans for the background and each measurement was set at 4 scans. This was followed by the determination of decomposition efficiency of toluene and m-xylene from NTP treatment by passing gas streams from NTP through the FTIR. Three spectra were recorded for each gas to obtain an average of gas concentration. The gas concentrations from the integrated area of the gas absorption band where then calculated by [20]:

$$N_{\text{ppm}} = \frac{INT_{\text{exp}} \times N_{\text{std}} \times L_{\text{std}}}{INT_{\text{std}} \times L_{\text{meas}}} \quad (1)$$

where N_{std}, L_{std} (given as 1 m), and L_{meas} represent the concentration of the standard gas produced by Infrared Analysis, Inc. and Pacific Northwest National Laboratories, optical path length of the standard gas measurement, and optical path length of the measured spectrum, respectively. The N_{std} for toluene and m-xylene were given as 100 ppm.

The destruction efficiencies of toluene and m-xylene were calculated by:

$$\eta(\%) = \frac{[\text{VOCs}]_{\text{inlet}} - [\text{VOCs}]_{\text{outlet}}}{[\text{VOCs}]_{\text{inlet}}} \times 100\% \quad (2)$$

2.3. Experimental design and optimization

The experimental design of toluene and m-xylene decomposition in a packed bed NTP reactor was done using Design Expert 7.0 (Stat-Ease, Inc., Minneapolis, MN, USA) software. CCD with three factors was chosen to design the experiment. This is because the three-factorial design offers an effective estimation of the second-order quadratic polynomials and gives the combination of values that optimizes the response within the region of the three-dimensional observation space [17]. The effects of three factors, namely applied voltage, discharge gap, and flow rate were studied. Each factor was varied over two levels: the high level (+1) and the low level (−1), usually referred to as the experimental domain. In order to define the experimental domain explored, results of preliminary experiments and previous studies were used [8,9]. Table 1 shows the selected experimental range for the three factors.

An experimental plan was generated based on these levels using the Design expert 7.0 software as shown in Table 2. This setup consisting of 20 experimental design runs in random order allows modeling of quadratic effects as well as main effects, and their interactions on the response variable.

In order to determine if a relationship exists between the factors and the responses investigated, the collected data was analyzed statistically using non-linear regression analysis. The responses can be expressed as second-order polynomial equations:

$$Y = \beta_0 + \beta_1 X_1 + \beta_2 X_2 + \beta_3 X_3 + \beta_{11} X_1^2 + \beta_{22} X_2^2 + \beta_{33} X_3^2 + \beta_{12} X_1 X_2 + \beta_{13} X_1 X_3 + \beta_{23} X_2 X_3 \quad (3)$$

where Y is the response (removal efficiency); X_1, X_2, and X_3 represent the three variables, respectively, and

Table 1
Selected experimental domain for each of the variables

Independent variables	Symbols	Levels	
		−1	1
Applied voltage (kV)	X_1	13	15
Discharge gap (mm)	X_2	20	30
Gas flow rate (L/min)	X_3	2.36	4.72

β_0, β_1, β_2, β_3, β_{11}, β_{22}, β_{33}, β_{12}, β_{13}, and β_{23} are the model coefficients calculated from the experimental data. The responses and variables were analyzed by the response surface function to obtain the values of the coefficients of Eq. (3) using Design expert 7.0 (Stat-Ease, Inc., Minneapolis, MN, USA) software.

The Design-Expert was also used for analysis of variance (ANOVA) and multiple regression analyses of the data obtained. The fit of regression model was checked by coefficient of determination R^2, Fisher's test F, and its associated probability p (at 95% confidence level) to determine the overall model significance. The significance of the respective independent variables on dependent variable was tested using the p-test and response surface plots. The model coefficients were determined via multiple regression analysis and the model equation was solved to determine the optimum operating variables.

3. Results and discussion

3.1. Modeling and statistical analysis

The experimental design and observed responses (performance removal efficiencies) are shown in Table 2. Analysis of those data using Design expert 7.0 gave the following quadratic regression models for performance removal efficiency of toluene in terms of the factors:

$$Y = 879.26 - 115.71X_1 - 1.33X_2 - 19.02X_3 + 0.4755X_1X_2 - 0.3178X_1X_3 + 0.24364X_2X_3 + 4.044X_1^2 - 0.14279X_2^2 + 1.51805X_3^2 \quad (4)$$

and for m-xylene

$$Y = 352.63 - 73.46X_1 + 13.72X_2 + 11.41X_3 - 0.394X_1X_2 + 0.534X_1X_3 - 0.316X_2X_3 + 3.2X_1^2 - 0.168X_2^2 - 1.957X_3^2 \quad (5)$$

where Y is the performance removal efficiency; X_1, X_2, and X_3 represent the values of applied voltage, discharge gap, and flow rate, respectively.

The response surface analysis allows the development of an empirical relationship in which the response variable (Y) was assessed as a function of applied voltage (X_1), discharge gap (X_2), and flow rate (X_3), both linear terms and various combinations of quadratic terms. The adequacy of the model was tested by ANOVA and additional purification experiments, such as optimization, using the Design Expert software. The results of the ANOVA for performance

Table 2
Experimental design as generated by Design expert 7.0 software and observed response (performance removal efficiency)

Run	Applied voltage (kV) X_1	Discharge gap (cm) X_2	Gas flow rate (L/min) X_3	Performance removal efficiency (%)	
				Toluene	Xylene
1	15.00	30.00	4.72	72.01	58.8
2	13.00	20.00	4.72	62.08	62.2
3	15.68	25.00	3.54	92.00	86.9
4	15.00	20.00	4.72	80.72	66.4
5	14.00	25.00	3.54	67.87	66.3
6	13.00	20.00	2.36	80.64	64.2
7	13.00	30.00	4.72	54.34	45.6
8	14.00	25.00	1.56	70.51	63.5
9	14.00	25.00	3.54	67.87	66.3
10	14.00	33.00	3.54	48.35	44.0
11	14.00	25.00	3.54	67.87	66.3
12	13.00	30.00	2.36	56.67	55.6
13	14.00	25.00	5.52	70.39	47.1
14	14.00	17.00	3.54	60.4	58.2
15	15.00	20.00	2.36	88.95	82.6
16	14.00	25.00	3.54	67.87	66.3
17	14.00	25.00	3.54	67.87	66.3
18	15.00	30.00	2.36	84.97	65.6
19	12.32	25.00	3.54	59.82	57.2
20	14.00	25.00	3.54	67.87	66.3

removal efficiency for toluene and m-xylene are shown in Tables 3 and 4, respectively. ANOVA provides the statistical results and diagnostic checking tests which enables the adequacy of the models to be evaluated [21]. It was found that the quadratic models were significant with probability of error (p) values of 0.0008 and 0.0001 for toluene and m-xylene, respectively. A value of p less than 0.05 indicates that a variable is statistically significant [22,23]. The Model F-value of 9.35 for toluene implies the model is significant and there is only 0.08% chance that a "Model F-value" this large could occur due to noise. Similarly, the Model F-value of 14.24 for m-xylene implies the model is significant and there is only 0.01% chance that a "Model F-value" this large could occur due to noise.

Tables 3 and 4 also show the F-values of each of the dependent variables, which is a measure of the significance of each variable in Eqs. (4) and (5), on the percentage removal of toluene and m-xylene. X_1, X_2, X_3, X_1^2, X_2^2, and X_3^2 with p-values of 0.0008, 0.0066, 0.050, 0.013, and 0.024, respectively are the significant model terms for toluene while X_1, X_2, X_3, X_1^2, and X_2^2 with p-values of 0.0001, 0.0002, 0.0014, 0.016, 0.0036, and 0.034, respectively, are the significant model terms for m-xylene. p-values greater than 0.1000 indicates the model terms are not significant. The values of the correlation coefficients (R^2) were found to be 0.89 and 0.93 for toluene and m-xylene, respectively. The R^2 coefficient gives the proportion of the total variation in the response predicted by the model, indicating ratio of sum of squares due to regression to total sum of squares. The R^2 value was found to be closed to the adjusted R^2 value of 0.80. A high R^2 value, close to 1, is desirable and a reasonable agreement with adjusted R^2 is necessary [19,24]. A high R^2 coefficient ensures a satisfactory adjustment of the quadratic model to the experimental data.

Adequate precision (AP) compares the range of the predicted values at the design points to the average prediction error. It measures signal-to-noise ratio. Ratios greater than 4 indicate adequate model discrimination [22]. AP values of 12.5 and 15.4 were obtained for toluene and m-xylene, respectively. The AP value, which is greater than four is adequate, and can be used to navigate the design space defined by the CCD. According to ANOVA, the AP value suggests that most of the differences in the response can be explained using the regression equation. The associated p-value is used to estimate, whether AP value is large enough to show statistical significance. If the p-value is lower than 0.05, it demonstrates that the model is statistically significant. The low standard deviation values of 5.12 for toluene and 4.21 for

Table 3
ANOVA for response surface of the model of toluene decomposition

Source	Sum of squares	df	Mean of squares	*F*-value	*p*-value prob. > *F*	Remark
Model	2,208.79	9	245.42	9.35	0.0008	Significant
A-applied voltage	1,181.76	1	1181.76	45.04	0.0001	Significant
B-discharge gap	306.19	1	306.19	11.67	0.0066	Significant
C-flow rate	130.91	1	130.91	4.99	0.0495	Significant
AB	45.22	1	45.22	1.72	0.2186	
AC	0.011	1	0.011	4.287×10^{-4}	0.9839	
BC	16.53	1	16.53	0.63	0.4458	
A^2	235.7	1	235.7	8.98	0.0134	Significant
B^2	183.63	1	183.63	7.0	0.0245	Significant
C^2	64.39	1	64.39	2.45	0.1483	
Residual	262.41	10	26.24			
Lack of fit	262.41	5	52.48			
Pure error	0.00	5	0.00			
$R^2 = 0.8938$						
Adj $R^2 = 0.7982$						

Table 4
ANOVA for response surface of the model of m-xylene decomposition

Source	Sum of squares	df	Mean of squares	*F* value	*p*-value prob. > *F*	Remark
Model	2,276.51	9	252.95	14.24	0.0001	Significant
A-applied voltage	920.36	1	920.36	51.81	0.0001	Significant
B-discharge gap	590.45	1	590.45	33.24	0.0002	Significant
C-flow rate	156.77	1	156.77	8.82	0.0140	Significant
AB	31.05	1	31.05	1.75	0.2156	
AC	3.18	1	3.18	0.18	0.6814	
BC	27.83	1	27.83	1.57	0.2392	
A^2	147.66	1	147.66	8.31	0.0163	Significant
B^2	254.52	1	254.52	14.33	0.0036	Significant
C^2	106.99	1	106.99	6.02	0.0340	Significant
Residual	177.65	10	17.76			
Lack of fit	177.65	5	35.53			
Pure error	0.00	5	0.00			
$R^2 = 0.9276$						
Adj $R^2 = 0.8625$						

m-xylene are also evidence that the quadratic model is seemingly the best for estimation removal efficiency of toluene and m-xylene in ferroelectric-packed bed NTP reactor. The coefficient of variance (CV) as the ratio of the standard error of estimated to the mean value of the observed response defines reproducibility of the model. A model normally can be considered reproducible if its CV is not greater than 10%. The results in Tables 3 and 4 also show that the regression linear and quadratic terms are significant, and the models are considered to be adequate in terms of reproducibility with CV value of 7.38 for toluene and 6.63 for m-xylene. The plots of predicted vs. actual experimental toluene and m-xylene percentage removal efficiency (Figs. 3 and 4) shows close to a straight line. This indicates good prediction of experimental data using the model. Actual values are the measured values for a particular experiment, whereas predicted values are generated using the approximating functions.

3.2. Process analysis

Visualization of the predicted model equation can be obtained by the response surface and contour plots. The response surface plot is the theoretical three-dimensional plot showing the relationship between the response parameters and the variables.

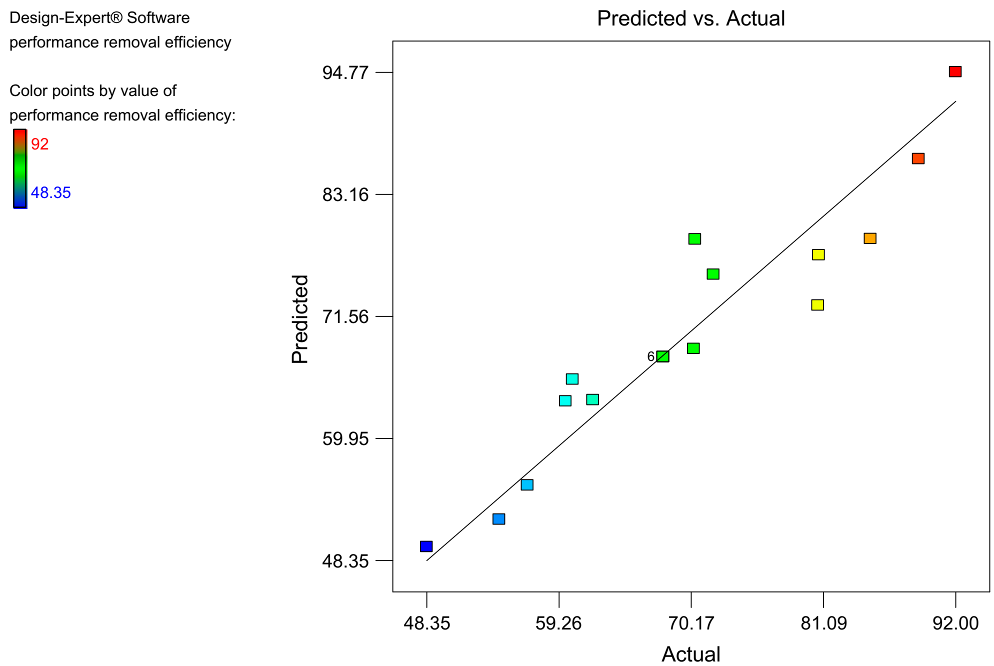

Fig. 3. Plot of predicted (%) vs. actual (%) response for toluene decomposition.

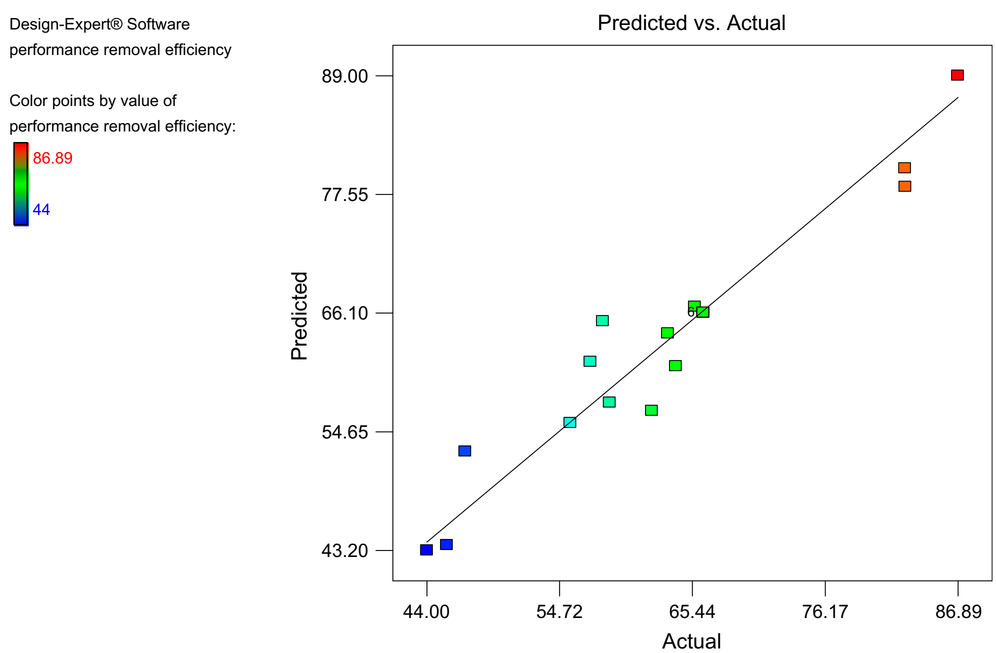

Fig. 4. Plot of predicted (%) vs. actual (%) response for m-xylene decomposition.

The two-dimensional display of the surface plot is called a contour plot. In the contour plot, lines of constant response are drawn in the plane of the variable. The contour plot helps to visualize the shape of a response surface. When the contour plot looks like an ellipse or a circle, the center of the system refers to a point of maximum or minimum response. Sometimes, contour plot may display hyperbolic or parabolic

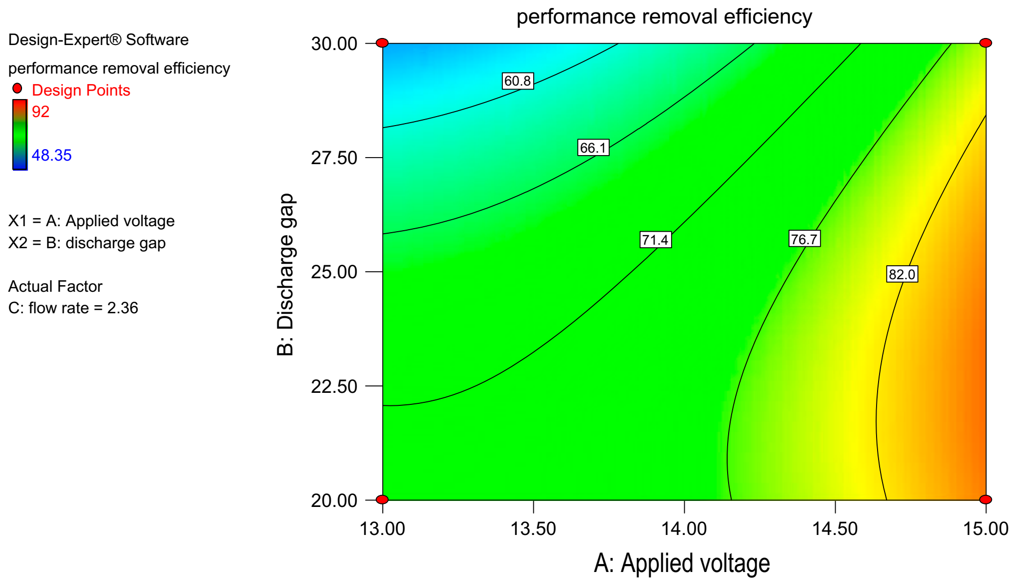

Fig. 5. Contour plot of applied voltage (kV) against discharge gap (mm) for toluene removal.

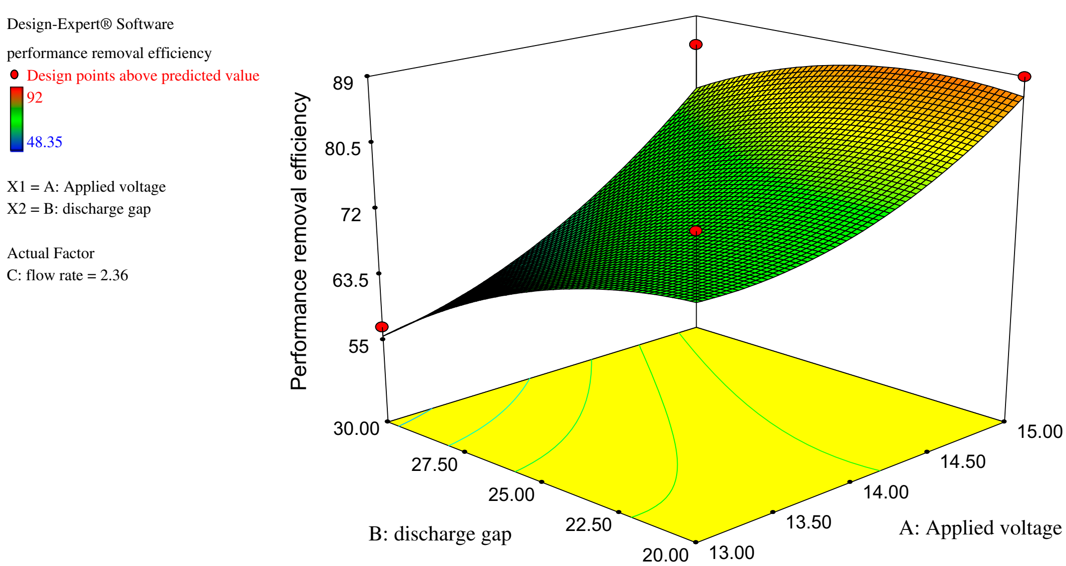

Fig. 6. Response surface plot for toluene removal efficiency (%).

system of the contours [25,26]. Contour plots supplied by RSM can illustrate the main and interactive effects of the independent variables on the response, and also help to confirm performance removal efficiency justification.

Figs. 5 and 6 depict the contour and response surface plots for the performance removal efficiency of toluene, respectively. The corresponding plots for m-xylene are depicted in Figs. 7 and 8. The figures show the changes in removal efficiency with varying applied voltage and discharge gap. It can be observed that increasing the applied voltage while reducing the discharge gap results in an increased performance of the NTP reactor for toluene and m-xylene removal. It is obvious that the optimal conditions for the removal efficiency were located in the region where the applied voltage is 15 kV and discharge gap is 20 mm. This can be attributed to the increased intensity of the plasma discharge observed as the applied voltage is increased. Also, it is reported that the electron density

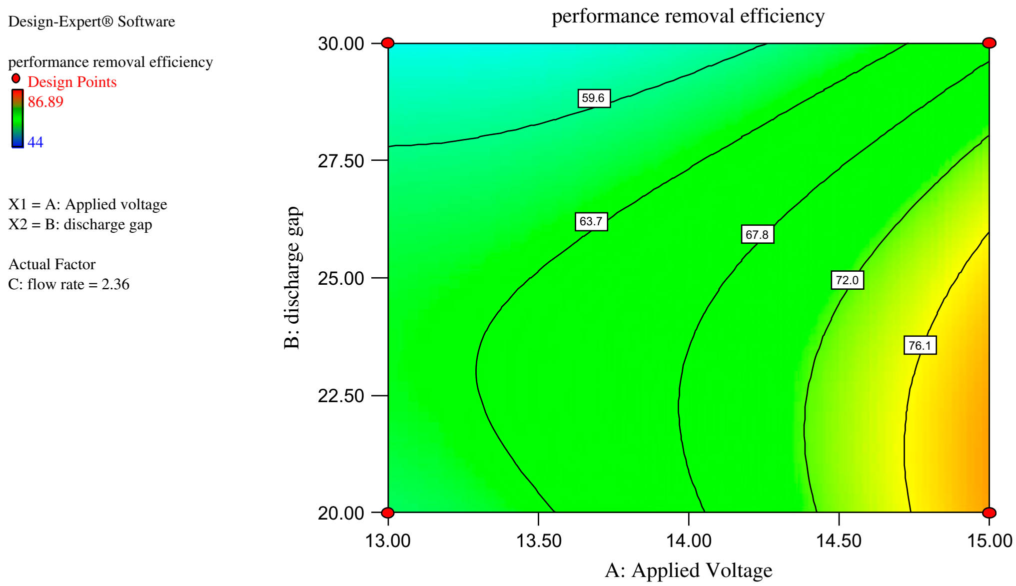

Fig. 7. Contour plot of applied voltage (kV) against discharge gap (mm) for m-xylene removal.

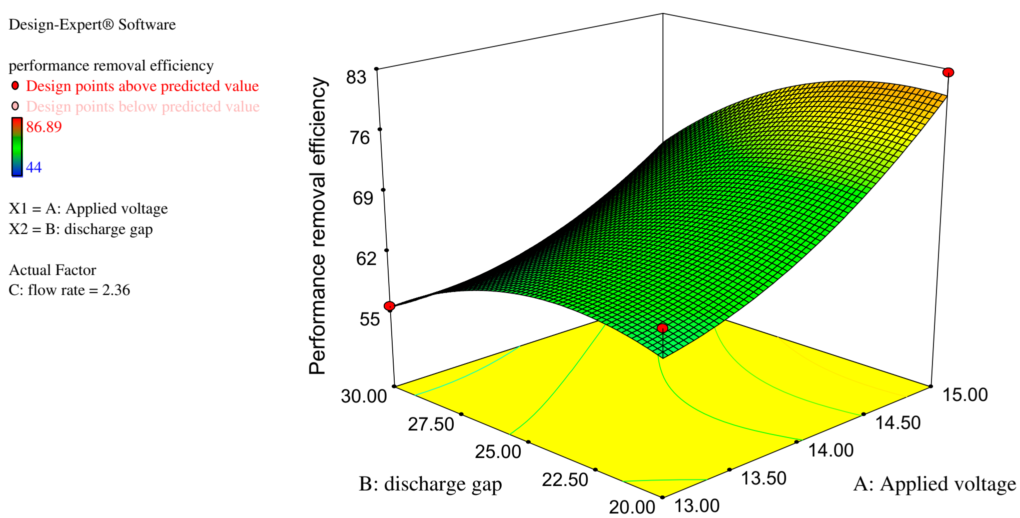

Fig. 8. Response surface plot for m-xylene removal efficiency (%).

increases with discharge current and voltage [11,27]. In addition, the electric field and mean electron energy get higher as the applied voltage is raised. Furthermore, when decreasing the length of the discharge gap, the maximum electric field and the total charge transferred by the microdischarges will increase. On the other hand, the residence time of the gas in the plasma region decreases when decreasing the gap length. Therefore, the response of a particular decomposition process will depend on which of these effects is more pronounced [28].

The effects of applied voltage can be further understood from the FTIR spectra for toluene and m-xylene in the gas sample before and after plasma treatment at 15.68, 14, and 12.32 kV, using a fixed discharge gap of 2.5 cm and flow rate of 3.54 L/min, respectively, as shown in Figs. 9 and 10. The residual toluene and m-xylene after treatment in NTP reactor decreases as the applied voltage is increased from 12.32 to 15.68 kV as seen from the spectral peaks.

The removal efficiency decreased from 92 to 59.827% as the applied voltage was reduced from

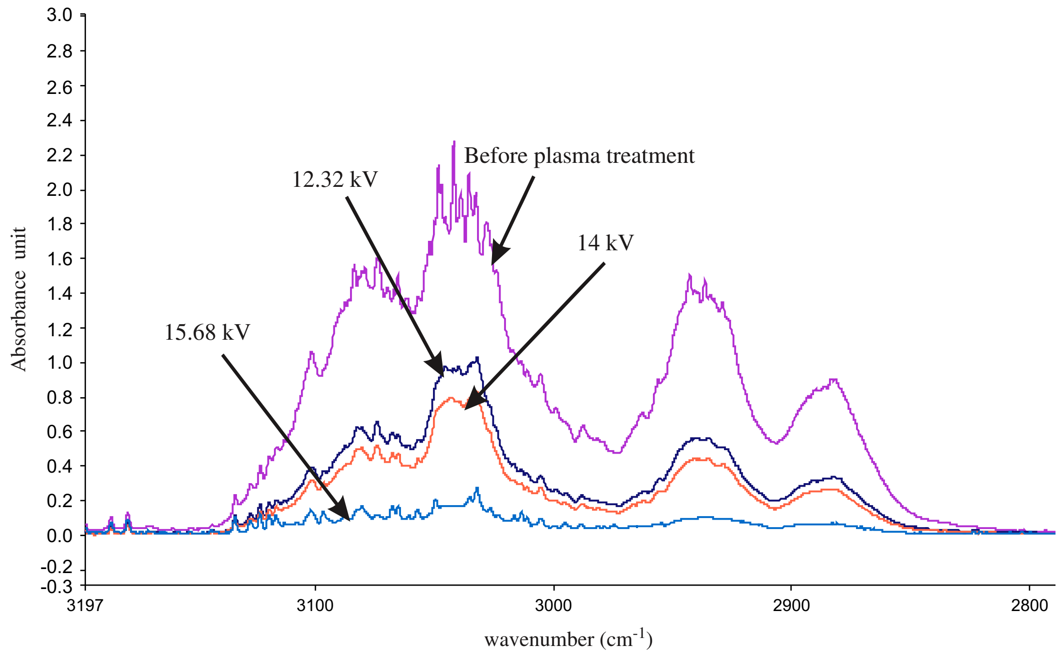

Fig. 9. FTIR spectrum of toluene decomposition at fixed discharge gap of 2.5 cm and flow rate of 3.54 L/min.

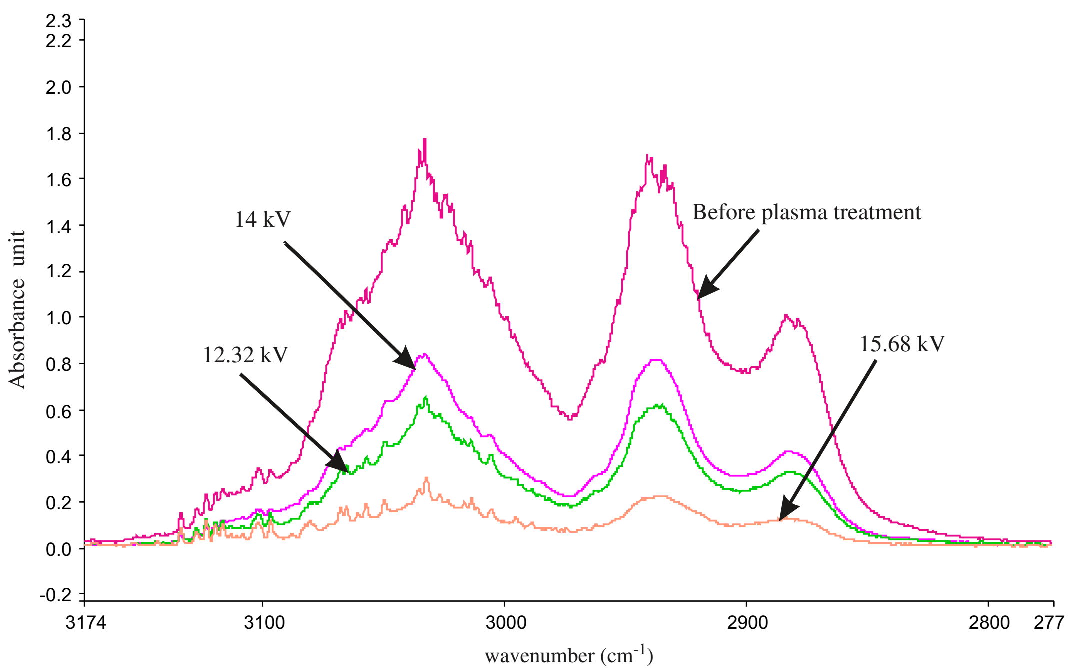

Fig. 10. FTIR spectrum of m-xylene decomposition at fixed discharge gap of 2.5 cm and flow rate of 3.54 L/min.

15.68 to 12.32 kV for toluene, while a decrease from 86.89 to 57.20% was observed for m-xylene, under the same condition. Numerical optimization was used to determine the optimum operating conditions for toluene and m-xylene removal. The optimum discharge gap, applied voltage, and flow rate for the decomposition were found to be 22.34 mm, 15 kV, 3.56 L/min and 20.10 mm, 15 kV, 3.34 L/min for

Table 5
Model prediction and actual removal

Parameter	Prediction	Actual	% error
Toluene removal efficiency (%)	87	86.2	1.2
m-xylene removal efficiency (%)	82	80.2	2.2

toluene and m-xylene, respectively. Experimental removal efficiencies and model predictions were in close agreement with 1.25 and 2.16% errors for toluene and m-xylene, respectively. The results are shown in Table 5.

4. Conclusion

An integrated air stripping and NTP system was employed in the treatment of toluene and m-xylene from wastewater. RSM was employed to analyze the interaction among the individual parameters. The optimum operating conditions for the decomposition of toluene and m-xylene in ferroelectric-packed bed NTP reactor were found to be 22.3 mm, 15 kV, 3.56 L/min and 20.1 mm, 15 kV, 3.34 L/min for toluene and m-xylene, respectively, for discharge gap, applied voltage, and flow rate, respectively, with a predicted toluene removal efficiency of 90%. Experimental removal efficiency and model prediction were in close agreement with values of 1.25 and 2.2% errors for toluene and m-xylene, respectively. It was concluded that the developed models could fit the experimental data with acceptable values of percentage errors.

Acknowledgments

The authors would like to express their sincere appreciation to Universiti Teknologi, Malaysia (UTM) for financial support under exploratory research grant scheme (ERGS); and to the former editor-in-chief of Water Science and Technology, Professor Gustaf Olsson of Lund University, Sweden and Guest Professor to UTM for reviewing the manuscript. Finally, we wish to thank Professor Koichi Takaki of Iwate University Japan for providing the barium titanate used for this research.

References

[1] A.H. Goldstein, I.E. Galbally, Known and unexplored organic constituents in the earth's atmosphere, J. Environ. Sci. Technol. 41(5) (2007) 1515–1521.

[2] R.G. Derwent, Sources, distributions and fates of VOCs in the atmosphere, in: R.E. Harrison, R.M. Hester, R.G. Derwent (Eds.), Volatile Organic Compounds in the Atmospheres, The Royal Society of Chemistry, UK, 1995, pp. 1–16.

[3] K. Inoue, H. Okano, Y. Yamagata, K. Muraoka, Y. Teraoka, Performance tests of newly developed adsorption/plasma combined system for decomposition of volatile organic compounds under continuous flow condition, J. Environ. Sci. 23 (2011) 139–144.

[4] J. Karuppiah, E. Linga Reddy, P. Manoj Kumar Reddy, B. Ramaraju, R. Karvembu, Ch. Subrahmanyam, Abatement of mixture of volatile organic compounds (VOCs) in a catalytic non-thermal plasma reactor, J. Hazard. Mater. 237–238 (2012) 283–289.

[5] T. Hammer, Application of plasma technology in environmental techniques, Contrib. Plasma Phys. 39 (1999) 441–462.

[6] M.E. Abdullahi, M.A. Abu Hassan, Z.N. Zainura, R.K. Raja Ibrahim, Volatile organic compounds abatement from industrial wastewater: selecting the appropriate technology, Aust. J. Basic Appl. Sci. 7 (2013) 103113.

[7] D.C. Montgomery, Experimental design for product and process design and development, The Statistician 48 Part 2 (1999) 159–177.

[8] G. Prieto, O. Prieto, C.R. Gay, T. Yamamoto, Destruction of residual fumigant using a plasma reactor, IEEE Trans. Ind. Appl. 39 (2003) 72–78.

[9] G. Prieto, M. Okumoto, K. Takashima, S. Katsura, A. Mizuno, O. Prieto, C.R. Gay, Nonthermal plasma reactors for the production of light hydrocarbon oleifins from heavy oil, Braz. J. Chem. Eng. 20 (2003) 57–61.

[10] T. Oda, K. Ono, R. Ono, Short gap non-thermal plasma performance to decompose dilute trichloroethylene, in: Proceedings of International Conference on Electrostatic Precipitation, ICESP X, Australia. Paper 5C1, 2006, pp. 1–10.

[11] A.M. Vandenbroucke, R. Morent, N.D. De Geyter, C. Leys, Non-thermal plasmas for non-catalytic and catalytic VOC abatement, J. Hazard. Mater. 195 (2011) 30–54.

[12] J.F. Xia, X.X. Gao, J.Y. Kong, H.X. Hui, M. Cui, K.P. Yan, By-products NO_X control and performance improvement of a packed-bed nonthermal plasma reactor, Plasma Chem. Plasma Process. 20 (2000) 225–233.

[13] T.K. Trinh, L.S. Kang, Response surface methodological approach to optimize the coagulation–flocculation process in drinking water treatment, Chem. Eng. Res. Des. 89 (2011) 1126–1135.

[14] H. Zheng, T. Tshukudu, J. Yang, Optimization of the coagulation–flocculation process for wastewatertreatment using polymeric ferric sulfate (PFS)-poly-diallyldimethyl ammonium chloride (PDADMAC) composite coagulant, Hydrol. Curr. Res. 3 (2012) 1–8, doi: 10.4172/2157-7587.1000139.

[15] J.M. Lucas, How to achieve a robust process using response surface methodology, J. Qual. Technol. 26 (1994) 248–260.

[16] S. Raisssi, Developing new processes and optimizing performance using response surface methodology, World Acad. Sci. Eng. Technol. 25 (2009) 1039–1042.
[17] M.S. Shehu, Z. Abdul Manan, S.R. Wan Alwi, Optimization of thermo-alkaline disintegration of sewage sludge for enhanced biogas yield, Bioresour. Technol. 114 (2012) 69–74.
[18] B. Lin, M. Jean, J. Chou, Using response surface methodology with response transformation in optimizing plasma spraying coatings, Int. J. Adv. Manuf. Technol. 34 (2007) 307–315.
[19] S.S. Madaeni, N. Arast, F. Rahimpour, Y. Arast, Fabrication optimization of acrylonitrile butadiene styrene (ABS)/polyvinylpyrrolidone (PVP) nanofiltration membrane using response surface methodology, Desalination 280 (2011) 305–312.
[20] R.K. Raja Ibrahim, Mid-Infrared Diagnostics of the Gas Phase in Non-Thermal Application, Unpublished PhD Thesis, University of Manchester Manchester, London, 2012.
[21] A. Talebi, T.T. Teng, A.F.M. Alkarkhi, I. Norli, L.W. Low, Optimization of nickel removal using liquid–liquid extraction and response surface methodology, Desalin. Water Treat. 47 (2012) 334–340.
[22] A. Malakahmada, S.Y. Chuan, Application of response surface methodology to optimize coagulation–flocculation treatment of anaerobically digested palm oil mill effluent using alum, Desalin. Water Treat. 51 (2012) 6729–6735.
[23] B.A. Nor Azimah, A. Mohd Ariffin, Z. Zainura, M.E. Abdullahi, B.J. Siti Fairuz, Optimization of the performance of chitosan for the nickel removal from wastewater, World Appl. Sci. J. 25 (2013) 1118–1124.
[24] S. Ghafari, H. Abdul Aziz, M.H. Isa, A. Zinatizadeh, Application of response surface methodology (RSM) to optimize coagulation–flocculation treatment of leachate using poly-aluminum chloride (PAC) and alum, J. Hazard. Mater. 163 (2013) 650–656.
[25] A.C. Affam, M. Chaudhuri, Optimization of Fenton treatment of amoxicillin and cloxacillin antibiotic aqueous solution, Desalin. Water Treat. 52(10–12) (2014) 1878–1884.
[26] M. Chaudhuri, H. Zuhali, A.C. Affam, Degradation of pesticide chlorothalonil by visible light-responsive photocatalyst ferrioxalate and under solar irradiation, Int. J. Photoenergy 2013 (2013) 1–7, doi: 10.1155/2013/435017.
[27] H.L. Chen, H.M. Lee, S.H. Chen, B.M. Chuang, Review of packed-bed plasma reactor for ozone generation and air pollution control. Ind. Eng. Chem. Res. 47(2008) 2122–2130.
[28] M. Magureanu, D. Piroi, N.B. Mandache, V.I. Parvulescu, Toluene oxidation in a dielectric barrier discharge combined with heterogeneous catalysis, Romania J. Phys. 56(Suppl. P) (2011) 156–162.